Numerical Analysis of Destruction Mechanisms of NPT- and FS-IGBTs in Forward Blocking Mode

U. Knipper, G. Wachutka
Institute for Physics of Electrotechnology
Munich University of Technology
Germany, Munich
knipper@tep.ei.tum.de

F. Pfirsch, T. Raker
Infineon Technologies AG
Germany, Munich
frank.pfirsch@infineon.com

***Abstract*—We studied different destruction modes of planar cell 1200V "Non-Punch-Through" and "Fieldstop" Insulated Gate Bipolar Transistors in Forward Blocking Mode using simulation tools. Branches of negative differential resistance are explained with certain device properties and a dynamic distortion of the electric field. Careful design of the device avoid these regions which may lead to current concentration and finally device destruction.**

I. Introduction

Achieving the largest possible safe-operating area (SOA) is a major concern in industrial applications. The SOA is determined by the maximum collector-emitter voltage and current within which the device operates without failure. The behavior and understanding of power devices at high voltages and high current densities are essential to extend the SOA.

The blocking characteristics are decisive for device ruggedness and provide a detailed insight in the critical operating states at the edge of the SOA. Power devices like Insulated Gate Bipolar Transistors are destroyed by thermal and/or electrical destruction [1]. Particular attention has to be paid to branches of the forward characteristics which exhibit negative differential resistance (NDR). Regions of NDR manifest themselves in a multifunction nature of the current-voltage characteristics and may result in current concentration and device destruction [2][3]. NDR branches may originate either from triggering the parasitic npn-transistor of the DMOS cell structure or from avalanche multiplication at the blocking pn-junction of the DMOS cell and the n-drift region/n-buffer layer, respectively.

II. Device Strucutres

A 1200V "Non-Punch-Through" Insulated Gate Bipolar Transistor and a 1200V "Fieldstop" Insulated Gate Bipolar Transistor (NPT-IGBT [4] and FS-IGBT [5]) are investigated. The NPT-IGBT has a thickness of 190 µm and a carefully designed p-body to avoid latching of the parasitic npn-transistor. The FS-IGBT is 120 µm thick and owns beside a carefully designed p-body an n-fieldstop layer for optimized breakdown voltage and injection efficiency. The FS-IGBT is studied with two different substrate doping concentrations, N_{Sub} (N_{Sub} = 7.5e13 cm^{-3} and N_{Sub} = 3.55e13 cm^{-3}, respectively).

III. 2D Device Simulation

We performed isothermal and electrothermally coupled quasi-stationary simulations of NPT-IGBTs and FS-IGBTs on the basis of a state-of-the-art multi-dimensional transport model implemented in DESSIS [6]. The forward blocking behavior of the analyzed devices are displayed in Fig. 1 (NPT-IGBT), Fig. 3 (FS-IGBT, N_{Sub} = 7.5e13 cm^{-3}) and Fig. 6 (FS-IGBT, N_{Sub} = 3.55e13 cm^{-3}), respectively. The isothermal

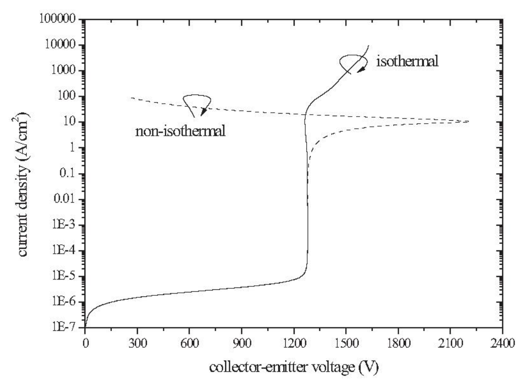

Figure 1. Forward blocking characteristics at 300 K for NPT-IGBT for different operating conditions.

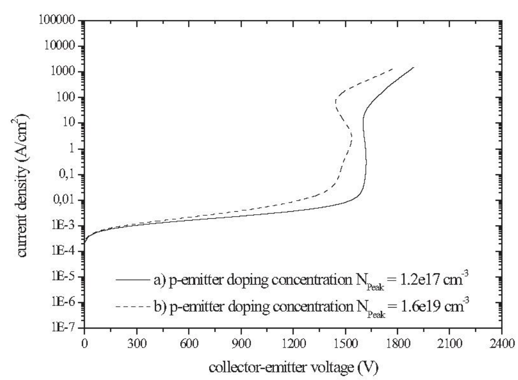

Figure 2. Forward blocking characteristics of the NPT-IGBT for various p-emitter doping concentrations (isothermal, 400 K).

 1-4244-0404-5/06/$20.00 © 2006 IEEE

TABLE I.
CALCULATED α_{PNP} OF THE NPT-IGBT FOR VARIOUS CURRENT DENSITIES AND TWO DIFFERENT P-EMITTER DOPING CONCENTRATIONS (CF. FIG. 2).

current density (A/cm^2)	*a) α_{pnp}*	*b) α_{pnp}*
0.15	0.72	0.95
1.5	0.51	0.90
15	0.34	0.59
150	0.36	0.40
1500	0.42	0.42

simulations serve as reference; they are based on an extended drift-diffusion model at constant temperature (300 K and 400 K, respectively). The fully coupled electro-thermal analyses are performed with the p-emitter kept at 300 K (ideal heat sink); heat and carrier transport are self-consistently simulated using an advanced electro-thermal model for high power devices.

IV. DISCUSSION OF SIMULATION RESULTS

A. NPT-IGBT (isothermal)

The isothermal simulations of the NPT-IGBT show almost no NDR behavior for low p-emitter doping concentration (Fig. 1). But higher p-emitter doping results in a significant NDR behavior, which is correlated with the common base current gain α_{pnp} (Fig. 2 and Table 1). For current densities above 10 A/cm^2, the electrons and holes generated by impact ionization attain concentrations, n and p, which become comparable to the doping concentration in the drift region, N_D, leading to a pronounced dynamic distortion of the electric field in the n-drift region. For $\alpha_{pnp} > 0.5$ the hole concentration exceeds the electron concentration in the n-drift region; consequently the slope of the electric field steepens resulting in a decrease of the voltage. A rule-of-thumb estimate of the voltage drop ΔV is given by [7]

$$\Delta V \propto \frac{N_D}{N_D + p - n} - 1$$

Hence, $p - n < 0$ leads to a decrease of the forward blocking voltage, $p - n > 0$ results in an increase. For $\alpha_{pnp} < 0.5$ the electron concentration exceeds the hole concentration and thus the voltage increases (Fig. 2 and Table 1).

B. FS-IGBT (isothermal)

Isothermal simulations of the FS-IGBT blocking characteristics with higher substrate doping concentration reveal two branches of NDR (Fig. 3). Increasing hole concentration in the p-body/n-drift region and a decreasing α_{pnp} ($\alpha_{pnp} < 0.5$) between the points marked as a and b in Fig. 3 are the cause of a steepening of the electric field profile in the p-body/n-drift region and a flattening of the electric field in the n-drift region. Moreover, the electric field is truncated by the action of the n-buffer layer (Fig. 4). All these effects together cause the voltage decrease from point a to point b. The concentrations of the generated carriers (Fig. 5) from point b to point c increases further on, exceeding now the doping level in the drift region and compensating each other almost to zero (i.e., plasma condition). As a consequence, the width of the neutral region becomes larger and the voltage increases accordingly from point b to point c. Along the branch from point c to point d, however, a second regime of impact

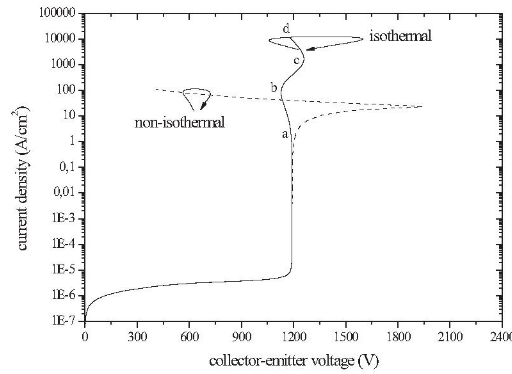

Figure 3. Forward blocking characteristics at 300 K for FS-IGBT with high substrate doping concentration ($N_{Sub} = 7.5e13\ cm^{-3}$) for different operating conditions.

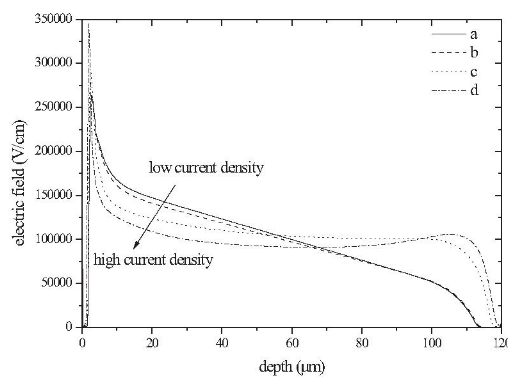

Figure 4. Electric field profile along a vertical cut through the FS-IGBT ($N_{Sub} = 7.5e13\ cm^{-3}$) for selected current densities.

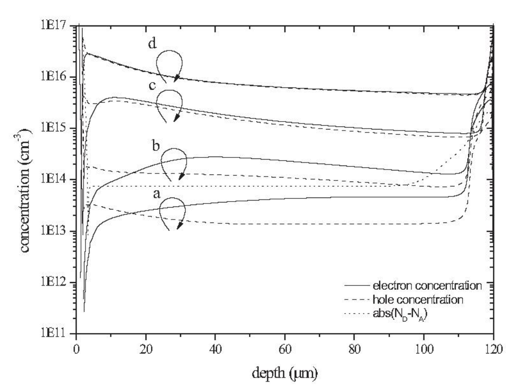

Figure 5. Generated carriers, n and p, along a vertical cut through the FS-IGBT ($N_{Sub} = 7.5e13\ cm^{-3}$) for selected current densities. N_D is the donator concentration and N_A the acceptor concentration through the device.

ionization develops in the n-buffer/n-drift region resulting in a "hanging" electric field profile sustaining a decreasing voltage.

The FS-IGBT with lower substrate doping concentration shows above current densities of about 1 A/cm^2 a continuously decreasing of the voltage (Fig. 6). Between the points marked as A and B in Fig. 6 the generated carriers become first comparable and then exceed the drift doping concentration (Fig. 8). The steepening of the electric field in the p-body/n-drift region due to the increasing hole concentration and the truncated electric field at the n-buffer layer (Fig. 7) cause a decreasing of the voltage. From point B to point C the voltage decreases further on due to similar reasons as in the FS-IGBT with higher substrate doping concentration: The generated carriers exceed now the doping concentration, compensate almost to zero and a second region of avalanche develops at the n-drift region/n-buffer layer resulting in a "hanging" electric. The main difference between the FS-IGBT with high and low substrate doping concentration is, that the space charge region of the FS-IGBT with low substrate doping concentration does not increase significantly and therefore the voltage does not increase. In industrial applications a continuous decreasing of the voltage may lead to a "jump" from the beginning of the NDR region at a certain current density to a region, where the differential resistance becomes once again positive at possible much higher current density. For large amplitudes of the "jump" the NDR region results in severe heating and finally in device destruction.

C. *Electrothermally Coupled Simulations of NPT-IGBT and FS-IGBT*

The self-consistent electrothermal simulations of the NPT-IGBT and the FS-IGBTs show similar behavior (Fig. 1, Fig. 3 and Fig. 6). Due to the local temperature rise in the vicinity of the DMOS cell, the impact ionization coefficients are degrading and, consequently, the voltage has to rise in order to maintain the carrier generation at the level necessary for keeping the current densities at about 10 A/cm^2. The maximum of the electron-current density and the maximum of temperature are still located in the center of the device. At a certain critical operating point, the parasitic npn-transistor turns on (Fig. 9), i.e., the n-source starts to inject electrons and becomes a dominant contribution. The electron diffusion current from the n-source increases due to two reasons: Because of thermal diffusion the temperature below the n-source starts to increase and due to the increasing voltage the voltage drop below the n-source at the p-body/n-drift region increases and therefore the multiplication rate [2]. After the electron-current from the n-source has become a dominant contribution the voltage starts to decrease and the maximum of the electron-current density and the maximum of the temperature are now located below the n-source. The controllability of the device is lost.

V. Conclusions

We find that the forward blocking characteristics of both NPT-IGBT and FS-IGBT may exhibit branches with NDR. In the case of the NPT-IGBT, NDR is primarily caused by a high common base current gain α_{pnp} ($\alpha_{pnp} > 0.5$). The FS-IGBTs show branches of NDR originating from an interplay of an excessive hole concentration in the p-body/n-drift region and a truncated electric field at the n-buffer associated with the occurrence of a second avalanche multiplication regime in the

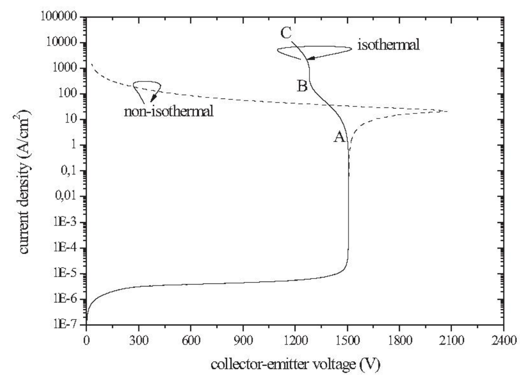

Figure 6. Forward blocking characteristics at 300 K for FS-IGBT with low substrate doping concentration (N_{Sub} = 3.55e13 cm^{-3}) for different operating conditions.

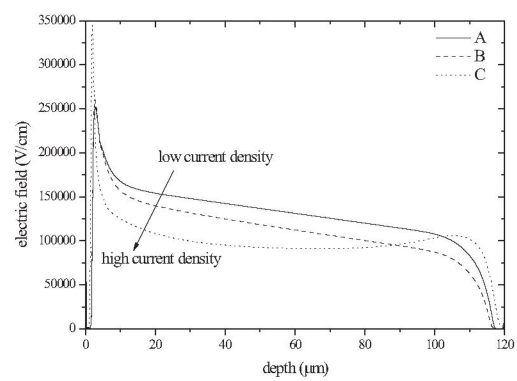

Figure 7. Electric field profile along a vertical cut through the FS-IGBT (N_{Sub} = 3.55e13 cm^{-3}) for selected current densities.

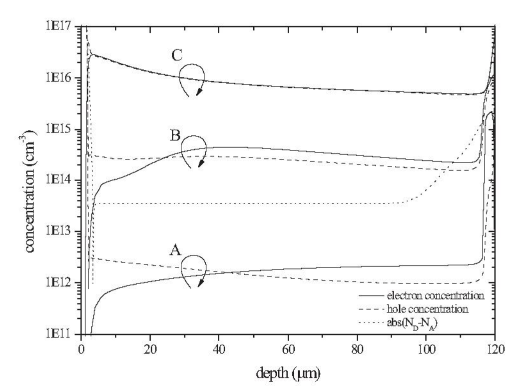

Figure 8. Generated carriers, n and p, along a vertical cut through the FS-IGBT (N_{Sub} = 3.55e13 cm^{-3}) for selected current densities. N_D is the donator concentration and N_A the acceptor concentration through the device.

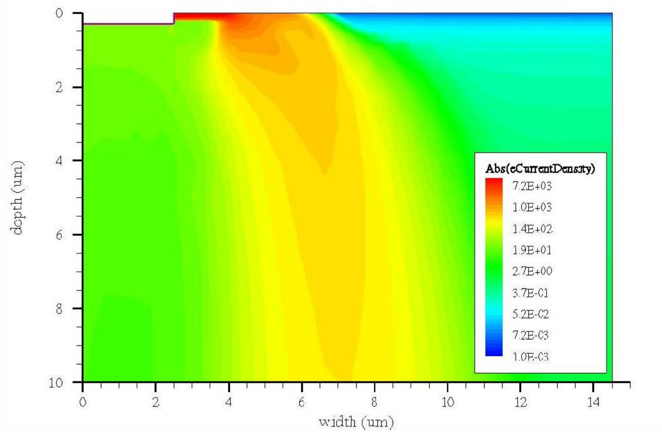

Figure 9. The electron-current density is crowding below the n-source after turn-on of the parasitic npn-transistor.

n-buffer/n-drift region.

As a major result of our study, we find that branches with NDR can be avoided by a careful design of the doping profile of the p-emitter and the n-buffer layer. The FS-IGBT with a lower substrate doping concentration shows certainly a higher breakdown voltage but at high current densities this device tends more to run away into destruction because of a continuously decreasing voltage.

REFERENCES

[1] H. Hagino, J. Yamashita, A. Uenishi, and H. Haraguchi, “An experimental and numerical study on the forward biased SOA of IGBTs”, IEEE Transactions on Electron Devices, vol. 42, pp. 490-500, March 1996.

[2] A. Icaza, G. Wachutka, F. Hirler, and J. Krumrey, “UIS-failure for DMOS power transistors”, ESSDERC 2002, Proceedings, pp. 459-462, September 2002.

[3] M. Shur, T. A. Fjeldly, H. Iwai, and J. Zolper, “Breakdown phenomena in semiconductors and semiconductor devices”, International Journal of High Speed Electronics and Systems, vol. 14, no. 4, p. 40, December 2004.

[4] J. Fugger, F. Hirler, T. Laska, and W. Scholz, “Optimizing the vertical IGBT structure – The NPT concept as the most economic and electrically ideal solution for a 1200V IGBT”, ISPSD 1996, Proceedings, pp. 169-172, 1996.

[5] T. Laska, M. Münzer, F. Pfirsch, C. Schaeffer, and T. Schmidt, “The Field Stop IGBT (FS IGBT) – A new power device concept with a great improvement potential”, ISPSD 2000, Proceedings, pp. 355-358, 2000.

[6] DESSIS TCAD, formerly distributed by Integrated Systems Engineering, Zurich, CH.

[7] S. Huang, K. Sheng, G. A. J. Amaratunga, F. Udrea, and P. Waind, “An experimental and numerical investigation of IGBT blocking characteristics”, PIEMC 2000, Proceedings, vol. 1, pp. 407-411, August 2000.

 1-4244-0404-5/06/$20.00 © 2006 IEEE